Terahertz Time-Domain Spectroscopy of Thermoresponsive Polymers in Aqueous Solution

Guillaume Serin,[†,‡] Hong Hanh Nguyen,[‡] Jean-Daniel Marty,[‡] Jean-Claude Micheau,[‡] Véronique Gernigon,[‡] Anne-Françoise Mingotaud,[‡] Damienne Bajon,[†] Thierry Soulet,[†] Sébastien Massenot,*[,†] and Christophe Coudret*[,‡]

[†]Institut Supérieur de l'Aéronautique et de l'Espace (ISAE-SUPAERO), Université de Toulouse, 31055 Toulouse Cedex 4, France
[‡]Laboratoire des IMRCP, Université de Toulouse, CNRS UMR 5623, Université Paul Sabatier, 118 route de Narbonne 31062 Toulouse Cedex 9, France

S *Supporting Information*

ABSTRACT: The behavior of highly concentrated aqueous solutions of two thermoresponsive polymers poly(N-isopropylacrylamide) (PNIPAm) and poly(N-vinylcaprolactam) (PVCL) have been investigated by terahertz time-domain spectroscopy (THz-TDS). Measurements have been performed for concentrations up to 20 wt %, over a frequency range from 0.3 to 1.5 THz and for temperatures from 20 to 45 °C including the zone for lower critical solution temperature (LCST). THz-TDS enables the study of the behavior of water present in the solution (i.e., free or bound to the polymer). From these measurements, in addition to phase transition temperature, thermodynamic data such as variation of enthalpy and entropy can be inferred. Thanks to these data, further

insights upon the mechanism involved during the dehydration phenomenon were obtained. These results were compared to the ones issued from dynamic light scattering, spectroscopy, or microscopy techniques to underline the interest to use THz-TDS as a powerful tool to characterize the behavior of thermoresponsive polymers in highly concentrated solutions.
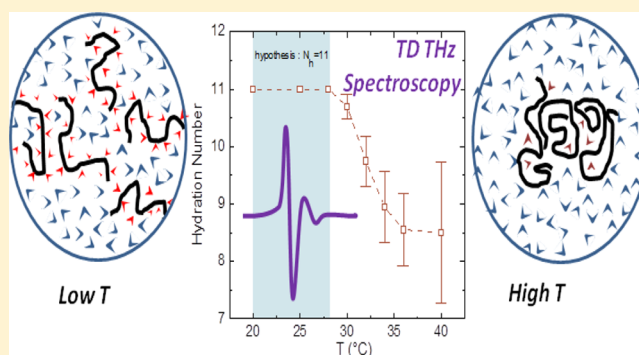
1. INTRODUCTION

Water-soluble polymers which have the ability to reversibly hydrate and dehydrate by simply changing the solution temperature have attracted significant attention since 1990.[1] Indeed, these materials can find applications in fields as various as drug delivery, sensing, catalysis, nanoelectronics, and so forth.[2] Poly(N-isopropylacrylamide) (PNIPAm) is by far the most commonly studied thermoresponsive polymer.[1] This preference is mainly related to its transition temperature around 32 °C, close to the body temperature and almost completely independent of the polymer chain length.[3] Among the other families of polymers presenting a transition temperature value close to the physiological temperature is poly(N-vinylcaprolactam) (PVCL),[4,5] also interesting for its moderate toxicity.

The transition temperature of these polymers corresponding to the solubility limit (i.e., when the solution becomes turbid) is called the "cloud point temperature" T_c. When T_c corresponds to the minimum observed on a temperature vs concentration phase diagram, it is also named the "lower critical solution temperature" (LCST). On these phase diagrams, different behaviors can be distinguished between the families of thermoresponsive polymers, depending on the evolution of

the cloud point with the polymer molar mass (type I or II)[3−6] and on the number of critical points (type III).[7]

Studying phase transition of thermosensitive polymers is crucial to their use, and this phenomenon is observable by monitoring the changes resulting from the modification of temperature at different length scales. First, the coil-to-globule conformational modification of the polymer in solution when T is increased above T_c induces changes at a macroscopic or microscopic scale. Thus, the behavior of these polymers in dilute solutions can be easily monitored optically by UV−visible spectroscopy,[8] turbidimetry,[6] and fluorescence spectroscopy,[6,9] whereas small angle neutron scattering (SANS),[10] nuclear magnetic resonance (NMR),[11] and dynamic light scattering (DLS)[12] provide information on the size and the mobility of the polymer. Nevertheless, studying the behavior of these polymers in highly concentrated aqueous solution appears as a more challenging task as most of these techniques are poorly adapted to such conditions. Differential scanning calorimetry (DSC) enables monitoring of the macroscopic heat flow exchanged by a polymer solution with a source during

phase transition which is correlated to enthalpy variation associated with polymer−water reactions.[5,13] The reorganization of the solvent and solute during the transition can also be probed by infrared spectroscopy. Hence, a change of the self-dissociation constant of water molecules in the vicinity of PNIPAm was reported, revealing a different solvent behavior depending on the presence of interactions with the polymer chain or with other water molecules.[14] Infrared spectroscopy results were also extended to the measurement of the polymer's C−H stretching evolution during phase transition for both PNIPAm and PVCL.[15]

Most of the previously mentioned techniques use the solute itself to probe its environment. However, the observed behaviors are far from simple; this is why more recent works enlarged the insights into the hydration dynamics of the macromolecules during their phase transition by directly studying the solvent in itself.[16] To go further into this way, characterization methods sensitive to hydrogen bonds and collective motions in water are needed. Microwave and terahertz (THz) dielectric spectroscopies have the ability to address such topics. Microwave dielectric spectroscopy is a now popular method, since polar solvents present dielectric relaxations in this frequency domain.[17] On the other hand, since benchtop THz spectrometers are now available, THz dielectric spectroscopy is experiencing a very fast rise. THz waves belong to one of the most unexplored spectral ranges, between 0.3 and 10 THz (wavenumbers between 10 and 333 cm^{-1} or wavelengths between 1 mm and 30 μm). Owing to the nature of THz waves which are very sensitive to subpicosecond processes and with the possibility to observe collective motions,[18,19] THz spectroscopy is particularly adapted to the analysis of water, as it presents a strong absorption coefficient over a large spectral window.[20] This absorption is intrinsically due to the water molecules' organization; therefore, this method is sensitive to any solute that could perturb or change the water behavior. As a consequence, the hydration of small molecules,[21] and mostly biologically relevant macromolecules, has already been studied.[14,22−25] Since thermosensitive phase separation is related to a change of hydration of polymer chains, THz spectroscopy is potentially suitable to monitor this phenomenon. Concerning PNIPAm, first studies in this spectral range were based on far-infrared spectroscopy[26] and more recently on attenuated total reflection THz time-domain spectroscopy.[27] In addition, microwave dielectric relaxation spectroscopy has also been used to study the hydration properties of PNIPAm[28,29] and PVCL.[30] Polymer solvation issues are typically addressed according to the temperature domains considered.

For temperatures below the cloud point temperature (namely, the "hydrophilic domain"), the organization of the solvent is considered to vary from "bulk water", far from the macromolecule, to "solvation water", close to the polymer. The contribution of this hydration layer to the absorption has been described as more complex than an ice-like approach, and needs deeper understanding as inter- and intramolecular hydrogen bonds are stronger close to the polymer−water interface, creating a blue shift and a behavior closer to cooled bulk water.[31,32] Interestingly, in order to get more information about this layer, one has to work on highly concentrated aqueous solution. Consequently, compared to most commonly used techniques that were best adapted for diluted solutions, THz spectroscopy is particularly adapted to the study of concentrated polymer solutions. Above the temperature-

induced demixing process, the main question will be to know how many free water molecules remain in the collapsed phase in addition to residual water directly bound to the solute. Finally, there is presently a lack of information to link routinely used techniques characterizing LCST phenomena to THz spectroscopy. In this work, we therefore investigate the behavior of aqueous solutions of two thermosensitive polymers, PNIPAm and PVCL (Figure 1), by transmission terahertz time-domain spectroscopy (THz-TDS).
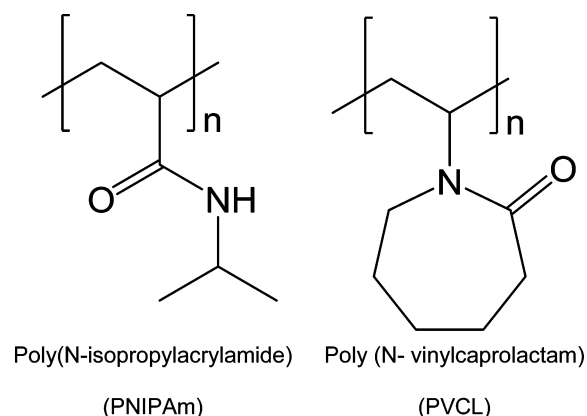

Figure 1. Chemical structures of PNIPAm and PVCL.

With a simple model of the dielectric properties of the solutions, we investigate to which extent THz spectroscopy enables confirming but also obtaining complementary results to the ones issued from most commonly used techniques. For this, we analyze the behavior of samples with different molecular weights, with mass fractions between 1 and 20 wt %, at temperatures from 20 to 45 °C, and over a frequency range from 0.3 to 1.5 THz.

2. MATERIALS AND METHODS

2.1. Sample Preparation. A set of three different number-averaged molar masses (2, 7, and 20 kg mol^{-1}, noted P2k, P7k, and P20k, respectively) of PNIPAm polymer was selected. P2k and P7k were commercially available (Aldrich), while P20k and PVCL with a number-averaged molar mass of 60 kg mol^{-1}, noted PVCL60k, were available from previous studies.[6,33] To compare the samples, we have chosen the temperature independent mass fraction W^P of polymer in the solution as defined in eq 1

$$W^P = \frac{m^P}{m^T} \tag{1}$$

with m^P being the mass of polymer and m^T the total mass of the solution. Aqueous solutions of different mass fractions (5, 10, 15, and 20 wt % for PNIPAm and 1 and 20 wt % for PVCL) (Table 1) were obtained by dissolving the appropriate amount of polymer in ultrapure water (Aquadem ρ = 18 MΩ·cm^{-1}). The names of the sample reflect the chain length and the mass fraction; for example, PNIPAm (7 kg mol^{-1}) with a concentration of 10 wt % is called P7K10.

2.2. Variable Temperature Terahertz Time-Domain Spectroscopy. Transmission measurements were performed on a Tera-K15 Kit THz-TDS setup from MenloSystems GmbH equipped with a Linkam THMS600 temperature controlled sample holder. THz absorption spectra of water-free polymers were recorded on neat polymer pellets. Solutions were put into

Table 1. List of Sample Names

polymer	$M_{\text{n theory}}$ (kg mol^{-1}) ($Đ^a$)	mass fraction (wt %)	sample names
PNIPAm	2 (1.2)	20	P2k20
PNIPAm	7 (2.2)	5	P7k5
		10	P7k10
		15	P7k15
		20	P7k20
PNIPAm	20 (1.3)	5	P20k5
		10	P20k10
		15	P20k15
		20	P20k20
PVCL	60 (1.2)	1	PVCL60k1
		20	PVCL60k20

^{a}Polydispersity index $Đ = M_w/M_n$, with M_w being the weight-average molar mass and M_n being the number-average molar mass.

rectangular fused 300 μm thick silica capillary tubes from Vitrotubes, thin enough to work in transmission mode (Figure 2). An empty capillary tube was used as a reference. The setup
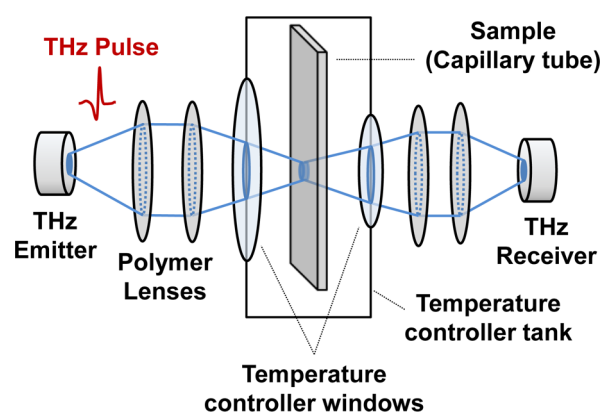

Figure 2. THz-TDS setup used in this study.

was placed in a dry atmosphere tank with a relative humidity (RH) lower than 5% in order to remove water vapor absorption. Samples were heated and then cooled with a heat flow of 1 °C/min over a temperature range depending on the polymer (20−40 °C for PNIPAm, 25−45 °C for PVCL). For

each experimental point, a plateau of 10 min at constant temperature was set. We used the first 90 s to let the solution stabilize thermally.

2.3. Parameter Extraction and Data Analysis. A measurement provides a time-domain pulse signal of several picoseconds proportional to the wave electric field. It is then possible to obtain two frequency-dependent data: the real part of the complex refractive index $n(f)$ and the absorption coefficient $\alpha(f)$ (in cm^{-1}) of the solution. By switching in the frequency domain, optical parameters $n(f)$ and $\alpha(f)$ were obtained from the magnitudes and phases of Fourier transforms of the signals in the frequency domain. In addition, the time-domain signals were truncated after the first main pulse to remove Fabry−Perot artifacts due to multiple reflections at window interfaces (Figure SI2.1). Three measurements for each sample were performed and averaged, and for the reference as well. Parameters extraction was made with the software Teralyzer from Lytera. The system characteristics allowed us to extract the absorption coefficient α over a range of 0.3−1.5 THz for each sample. As an example, a sample of ultrapure water was analyzed and our results were consistent with the literature (Supporting Information, section 3).

An "ideal" absorption coefficient α^{ideal} (or "two-component model") was obtained by adding the contribution of both pure components weighted by their mass fractions (eq 2)[30]

$$\alpha^{\text{ideal}}(f, T) = W^{\text{H}_2\text{O}}\alpha^{\text{H}_2\text{O}}(f, T) + W^{\text{P}}\alpha^{\text{P}}(f, T) \qquad (2)$$

where $W^{\text{H}_2\text{O}}$ stands for the water mass fraction as defined in eq 1. $\alpha^{\text{H}_2\text{O}}(f, T)$ and $\alpha^{\text{P}}(f, T)$, expressed in cm^{-1}, are the absorption coefficients, respectively, of pure water and pure polymer at temperature T and frequency f. Eventually, to the experimental α^{obs} was subtracted α^{ideal}. This difference is labeled $\Delta\alpha$ (eq 3).

$$\Delta\alpha(f, T) = \alpha^{\text{obs}}(f, T) - \alpha^{\text{ideal}}(f, T) \qquad (3)$$

3. RESULTS

3.1. Study of PNIPAm Solutions at 25 °C. In this work, we will focus on the absorption coefficient which provides more contrast with temperature than refractive index. THz-TDS measurements were performed on the different samples involving both PNIPAm and PVCL polymers (Figure 1). The
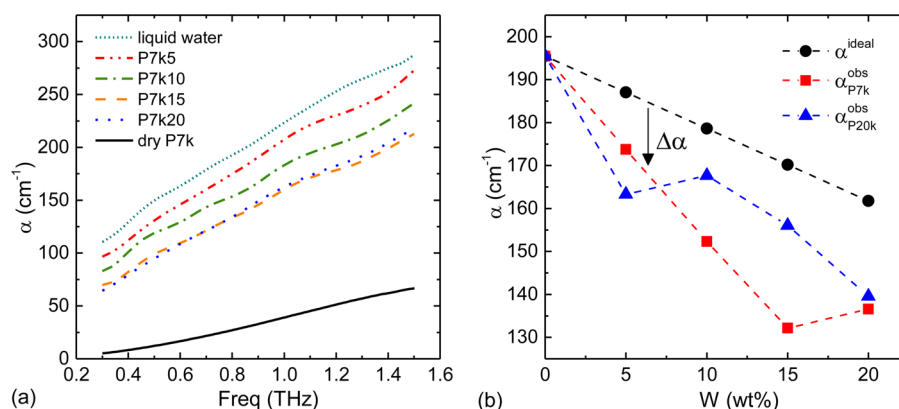

Figure 3. (a) Absorption coefficient from samples P7k5, P7k10, P7k15, and P7k20 compared to bulk liquid water and dry P7k at 25 °C. (b) Absorption coefficient at 0.8 THz vs polymer concentration (experimental results at 25 °C for P7k (red ■) and P20k (blue ▲)); black ● represent calculated results assuming an ideal two-component model from eq 2 for both P7k and P20k, as their coefficient in the dry state has the same value. The 0.8 THz frequency was chosen for its better signal-to-noise ratio. Lines are guides for the eyes.
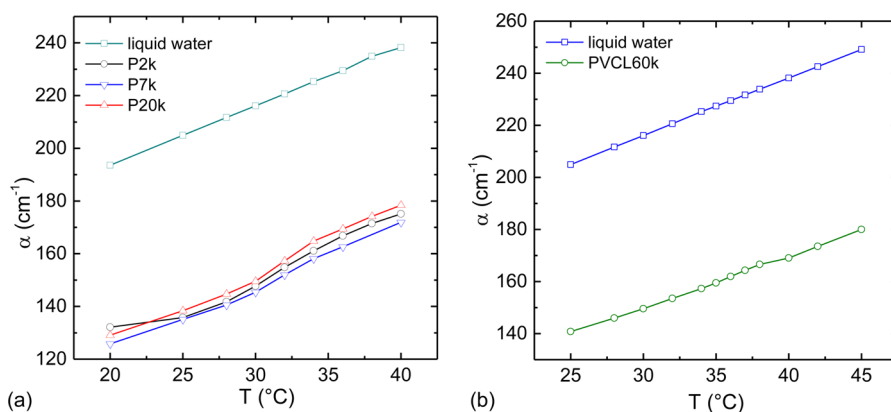
Figure 4. Comparison of absorption coefficient for (a) different chain lengths of PNIPAm and (b) PVCL at 0.8 THz and for a constant mass fraction of 20 wt % during the heating process. Lines are guides for the eyes.

influence of polymer concentration on the absorption coefficient was first examined on a single polymer, namely, P7k. Besides, pure liquid water was also studied, as well as pellets of dry P7k. The absorption coefficient was inferred from the initial spectra and is reported in Figure 3a. As expected, the absorption coefficient decreased as the polymer concentration increased (Figure 3a). Figure 3b shows the absorption coefficient at 0.8 THz vs polymer concentration. Calculated results for the ideal two-component model are also reported on the same graph. The difference $\Delta\alpha$ between the observed and calculated absorption coefficients is the signature of the polymer/water interaction. Its variation vs the nature of the polymer and the temperature (at a given frequency and concentration) was thus subsequently investigated.

3.2. Characterization of the Phase Transition for PNIPAm and PVCL. THz-TDS measurements were performed on 20 wt % solution of PNIPAm with different molar masses while the temperature was increased from 20 to 40 °C. The absorption coefficient at 0.8 THz is reported for the different polymers as a function of temperature in Figure 4a. For all PNIPAm samples, the relation between the absorption coefficient and the temperature exhibits a sigmoidal shape due to the phase transition occurring at the cloud point. The inflection point of this curve was used to determine the cloud point value (Supporting Information, section 4). T_c was found at 32.1, 32.2, and 31.3 °C on heating for P2k20, P7k20, and P20k20, respectively, and thus is independent of the polymer length. The same experiments performed in the case of PVCL enabled the determination of a characteristic temperature of 36.4 °C on heating. In the literature, PVCL has been shown to exhibit a "classical" Flory−Huggins thermoresponsive phase behavior in water,[4] with the position of the critical point depending on the concentration and chain length. As a type I polymer, in a temperature vs concentration phase diagram, this critical point shifts to a lower polymer concentration value as the chain length increases. It eventually tends to a zero concentration if the molar mass goes to infinity while the critical temperature transition tends to the so-called "θ temperature" (this Θ state represents the critical point at which the polymer chain exhibits its lowest dimension while remaining soluble).

Measured temperatures on cooling were found at 28.8, 30.8, 31.1, and 34.6 °C for P2k20, P7k20, P20k20, and PVCL60k20, as shown in Figure 4. A small hysteresis was observed which is inherent to the hydration process of thermoresponsive

polymers.[3] Comparing the shape of the curves in Figure 4a and b already provides interesting information. Whereas the evolution of α with the temperature for PNIPAm clearly exhibits a sigmoid shape, this is not the case for PVCL, presenting only a small mark through LCST. Before going further into THz analysis, this is already proof that both polymers do not exhibit the same dehydration process.

The variation of $\Delta\alpha$ vs the nature of the polymer and the temperature (at a given frequency and concentration) was then used to investigate the signature of the polymer/water interaction. Two samples of PNIPAm and PVCL with an equal mass fraction of 20 wt % (P7K20 and PVCL60K20) were compared. Results are reported in Figure 5 at 0.8 THz.
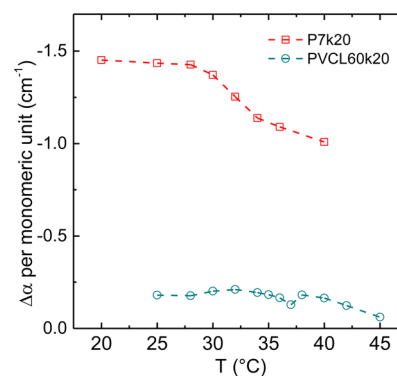

Figure 5. Contribution of the solvation water to $\Delta\alpha$ per monomeric unit for PNIPAm P7K and PVCL 60K at 20 wt %, during the heating process. Values presented here are calculated from eq 7 at 0.8 THz. Lines are guides for the eyes.

Whereas a sharp transition was exhibited by PNIPAm around 32 °C, a quasi-constant smooth evolution of the VCL monomer contribution to the absorption properties of the sample was observed (lower than the uncertainty of the instrument). This observation has also been reported by Hou et al. with Fourier-transformed infrared spectroscopy (FTIR) measurements.[15] This result is related to the different phase transition mechanisms for these two polymers. It is likely that during the phase transition there was a significant water reorganization around PNIPAm, while in PVCL the reorganization occurred gradually for temperature $T > T_c$.[6] This difference is mainly ascribed to the ability of monomers from PNIPAm to interact through hydrogen bonding after

dehydration. In the case of PVCL, such an interaction is no longer possible: the collapse of the polymer chains generates mesoglobules stabilized against further aggregation via the hydrophilic surface. Upon increasing temperature, this structure can further expel water molecules, progressively leading to the formation of aggregates of increasing size. This two-step dehydration phenomenon is also evidenced on thermograms where transition peaks present a highly asymmetric profile.[6] $\Delta\alpha$ is therefore an excellent parameter, showing the existence of the LCST, even on systems which do not present a clear sigmoidal evolution of α. It also has the ability to enlighten different transition mechanisms.

3.3. Study of the Solvation Water Bound to the PNIPAm Molecule. As already explained, around the LCST, the polymer chain/water interaction is modified, leading to a local then generalized dehydration process, producing a macroscopic precipitation. Necessarily, this phenomenon happens with a decrease of the number of water molecules around each monomer unit. Therefore, analyzing hydration dynamics and determining the hydration number is also relevant for the characterization of the process.

However, it is hard to separate the solvation shell layer from the bulk water without any hypothesis. Because the PNIPAm hydration number at $T < T_c$ is better described in the literature than PVCL and because P7K samples exhibited a linear behavior on α vs the mass fraction graph for $W \leq 15$ wt % (Figure 3b), we will focus on samples P7K5, P7K10, and P7K15 to propose a methodology to study the solvation water for the diluted regime. The structuration of water by the solute defines a new type of behavior of the water molecule, different from the bulk one and responsible for the modified absorption compared to the simple addition of the two-component contributions (Figure 3b). This result has already been observed by THz spectroscopy of the aqueous solution of biomolecules.[16,25,34] This leads to distinguishing two kinds of water for analyzing data (eq 4)

$$W^{H_2O}(T) = W^B(T) + W^S(T) \tag{4}$$

where W^B and W^S stand, respectively, for bulk water and solvation water, and the mass conservation is given by eq 5.

$$1 = W^B(T) + W^S(T) + W^P \tag{5}$$

Thus, a three-component model is used for α^{obs}, given by eq 6

$$\alpha^{obs}(f, T) = W^B(T)\alpha^B(f, T) + W^S(T)\alpha^S(f, T) + W^P\alpha^P(f, T) \tag{6}$$

The difference $\Delta\alpha$ between the two models is given by eq 7:

$$\Delta\alpha(f, T) = W^S(T)(\alpha^S(f, T) - \alpha^B(f, T)) \tag{7}$$

We assumed that the contribution of the polymer is identical to the dried polymer one. In the literature, the hydration number N_h of the PNIPAm molecule is commonly estimated between 8 and 13.[28,35,36] We thus used an averaged $N_h = 11$ water molecules per monomer NIPAm at $T < T_c$ as the hypothesis. Then, the mass fractions of both solvation water W^S and bulk water W^B in the solutions were estimated by using eq 8 and the conservation of the mass

$$W^S(T) = \left[N_h(T)\frac{M_{H_2O}}{M_{IPAm}}\right]W^P \tag{8}$$

where M are molar masses in g mol^{-1}. Once W^S is known, the absorption coefficient of the solvation water can be obtained from eq 7:

$$\alpha^S(f, T) = \frac{\Delta\alpha(f, T)}{W^S(T)} + \alpha^B(f, T) \tag{9}$$

In the same manner, the solvation water spectrum was estimated at $T = 20$, 25, and 28 °C during the heating process, as we observed a stable hydration dynamics in this temperature range for PNIPAm (Figure 5). From these results, we assumed a linear evolution of the absorption coefficient of the solvation water when the temperature increased (Figure S12). After this step, the solvation water absorption coefficient for higher temperature was extrapolated with linear regression (Figure S13).

Finally, the solvation water mass fraction at temperatures higher than the cloud point was estimated from the extrapolated absorption coefficient of the solvation water (eq 9). Then, an estimation of the hydration number N_h was carried out for the heating (eq 10).

$$N_h(T) = \frac{M_{IPAm}}{M_{H_2O}}\frac{W^S}{W^P} \tag{10}$$

The results show that ca. 3 water molecules were expelled from the polymer solvation shell of PNIPAm (Figure 6). As
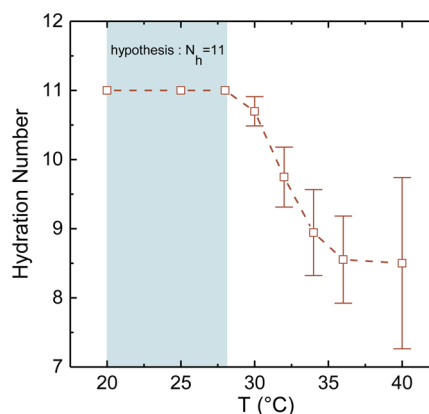

Figure 6. Hydration number for polymer P7k in aqueous solution concentrated at $W \leq 15$ wt %, based on a hypothesis of $N_h = 11$ until $T = 28$ °C before the phase transition (Supporting Information, section 5). At a given temperature, we calculated N_h from the absorption coefficient α_i^{obs} observed at each frequency data point from 0.3 to 1 THz, where i is P7k5, P7k10, or P7k15, respectively. Because the hydration number does not vary highly with mass fraction and frequency, we represent the average value of all N_h results from the three studied samples at each temperature $T > 28$ °C. Error bars represent the standard deviation at 1 sigma. Lines are guides for the eyes.

shown in Figure 5, PVCL is less sensitive to the temperature variations; therefore, the variation of the hydration number cannot be reached accurately. The evolution of the hydration number at a temperature higher than the cloud point is still challenging.[37] However, our results show that a substantial quantity of water molecules remains bound to the polymer after the phase transition, close to the five expelled water molecules per NIPAm monomer reported in the literature.[36] PNIPAm has been reported to have a different behavior than its monomer

unit regarding hydration dynamics,[37] suggesting a stronger influence on the water network of the polymer chain.

4. DISCUSSION

Several points are noteworthy regarding the method proposed in this work. First, compared to other studies of the literature, the THz spectrometer used is commercially available, with its drawback being a limited spectral range of analysis (0.3−1.5 THz due to a simple transmission setup allowing an easier extraction of the absorption coefficient). Indeed, water is known to exhibit absorption bands at 6 and 20 THz, which have been respectively attributed to hydrogen bond stretching vibrations and hindered rotational motions (Figure S3).[16] Interestingly, the band at 6 THz has been shown to be the signature of stretching motions of the first shell of hydration by *ab initio* molecular dynamics (AIMD).[39] It would therefore appear as more relevant to characterize solvation processes by analyzing the evolution of these bands. This has been done by Havenith's team in a very efficient manner, leading, for instance, to characterization of glycine or protein solutions. To be more specific, ref 39 emphasized the influence of the radius of the hydration shell to the far-IR absorption of solvated water molecules, and compared it to bulk water. This however implies the use of THz sources that cannot be easily commercialized at this point. Our study shows that, even with a basic THz spectrometer, some information can be gathered, even if it is not as thorough as those obtained from advanced spectrometers. The reason for this can be attributed to the fact that the THz water spectrum around 2.4 THz is mainly governed by a motion of the second hydration shell, providing an important contrast with bulk water at this frequency.[38] It can be assumed that the signature of this motion extends up to lower THz frequencies, leaving traces at the THz range studied here. It means that the water molecules that we are able to detect in our work are mainly those located in the hydration shell as a whole, without discrimination of the precise position of water molecules from the polymer, and the absorption coefficient of the solvation water is expected to be lower than the bulk water one in the frequency range reported in this study,[38] which is consistent with our results. Since THz spectroscopy probes the state of water molecules in the hydration layers, the importance of concentration is pertinent. Indeed, Havenith has shown that the THz absorption coefficient behavior of a biomolecule solution first cannot be simulated by a simple two-component model and that it highly depends on its concentration. Figure 3b also illustrates this, with the upper points being the two-component model. Regarding the influence of concentration, Havenith showed that, whereas a linear dependence of the absorption coefficient against concentration has been observed for diluted solutions, deviation from linearity is observed for concentrated ones. This has been explained by the overlapping of hydration shells for high concentrations.[16] In our case, the plateau obtained for the variation of α^{obs} in Figure 3b could be attributed to this behavior. Overlapping of the hydration shell should be corroborated to the critical overlap concentration $C*$ of polymer chains,[39] which is defined as

$$C* = \frac{3M_{\mathrm{w}}}{4\pi R_{\mathrm{g}}{}^{3}N_{\mathrm{A}}} \tag{11}$$

with M_{w} being the weight-averaged molar mass, R_{g} its radius of gyration, and N_{A} Avogadro's number and $C*$ units being g·L^{-1}.

For P7k, this concentration $C*$ can be estimated around 131 g·L^{-1}, corresponding to a mass fraction of PNIPAm of $W* = 12$ wt % assuming a radius of gyration in water at 20 °C of 2.9 nm.[40] For P2k, $W*$ is estimated around 22 wt % and was therefore not reached under our conditions. Finally, in the case of P20k, $W*$ is estimated around 6 wt %. These results perfectly fit with the mass fraction influence on the absorption coefficient in Figure 3b.

4.1. Comparison of THz-TDS to Other Techniques for Studying LCST. The second point that can be discussed is the comparison of LCST determination by THz spectroscopy compared to other routinely used techniques, such as DLS, DSC, or turbidimetry. As presented above, the determination of cloud point temperatures was performed from the graph reporting absorption coefficient as a function of temperature. The obtained values are in good agreement with the ones reported in the literature.[3] A comparison of THz and DSC values is provided in the Supporting Information (Table S1). It is noteworthy that, in Table S1, the cloud point was determined by DSC using the top of the peak corresponding to the transition. All results are consistent, with the maximum difference between both techniques being less than 2.5 °C. This shows that DSC and THz spectroscopy lead to the same characterization of the process at a similar time scale. Indeed, as already explained, THz provides information on the solvation in the first two hydration layers. This is very local information and modification of this layer may start early in the process, but a critical ratio of modified interaction has to be reached before detection by the method. On the other hand, DSC analyzes the energy provided by the breaking of hydrogen bonds. This is also very local and starts early in the transition process. Measuring the position of the transition from the maximum of the peak reveals the time when the phenomenon is at its maximum. Differences between both techniques are however linked to the speed of analysis. DSC is routinely performed using a temperature ramp which has to be regular, even if slow. No plateaus can be made on the ramp, since this would lead to artifacts on the thermograms due to stabilization of the instrument. This is why several temperature programs were used here in DSC at different rates, followed by the extrapolation at zero speed.

For THz spectroscopy, the situation is reverse. The temperature during spectrum recording should be stable, and therefore, temperature programs with a plateau at each temperature were used (Supporting Information, section 4.1). The small difference between DSC and THz results might be attributable to this method difference.

Supporting Information sections 4.3 and 4.4 also provide the characterization of the polymer solution LCST by turbidimetry and DLS, respectively. Turbidimetry showing the absorbance of the solution as a function of temperature highlights specific problems of the method when dealing with concentrated solutions. A strong hysteresis was observed for all solutions (Figure S10), owing to the slow response of aggregates in concentrated solutions to rehydrate and redissolve. This is expected for concentrated solutions of PNIPAm owing to the existence of possible intramolecular hydrogen bonds. DLS on the other hand measures the scattered intensity fluctuation of the solution. From these, the intensity of the scattered light is measured and the size of the scattering object evaluated. Typical results are presented in Figure S11. On these, the size was observed to strongly increase around 26 °C, but the analysis became erratic and not satisfactory. This is not

surprising, since DLS can only analyze solutions of non-flocculating objects, the size of which should not be larger than a few hundreds of nanometers. For turbidimetry and DLS, the values of T_c were found to be lower by a few degrees (typically 2−3 °C), either on heating or cooling, compared to those obtained by THz-TDS and DSC. This behavior is expected using DLS, since the presence of only a few aggregates will be detected by the technique, with the scattered intensity being linked to the molar mass of the scattering object to the power of 6. Turbidimetry is also based on light scattering, since this is at the basis of transmittance decrease. Therefore, it also shows the LCST process at a very early timing. Interestingly, whereas determination of cloud point by using DSC peak tops matches that found by THz spectroscopy, the use of DSC peak onsets matches the results found by turbidimetry and DLS.

Microwave and THz dielectric spectroscopies are particularly suitable to study highly concentrated aqueous solutions. Indeed, since they are sensitive to collective motions of water molecules, they are strongly absorbed by the solvent. The study of highly concentrated solutions (containing less water) allows obtaining a better signal-to-noise ratio while keeping a good sensitivity to the presence of hydration water. PNIPAm has been especially investigated by Füllbrandt et al.[29] in the microwave spectral band, which shows two dielectric relaxations, one around a few MHz corresponding to reorientation of hydrated polymer dipoles and a second around 19−20 GHz corresponding to the reorientation of water molecules. They estimated a number of 5 molecules per monomer unit released during the LCST. With a simple model based on the absorption coefficient of the solution, this work estimates that 3 molecules are released at LCST with THz-TDS; this result is coherent with the literature where 2.5 molecules[41] or 3.5 molecules with ATR THz-TDS and a model based on the bulk water behavior.[27] Eventually, it is interesting to note that the chain length has no significant effect on the observed cloud point of the PNIPAm polymer. This is consistent with the literature showing that the PNIPAm molecule exhibits a type II behavior.[3] Type II thermoresponsive polymers necessitate the introduction of a strong, concentration-dependent polymer−solvent interaction function in the expression of the Flory−Huggins theory. The position of the critical point in a temperature vs concentration phase diagram does not shift to 0 with increasing molar mass and is almost independent of the polymer chain length.[3] This is also consistent with dielectric spectroscopy results of Füllbrandt et al.[29]

4.2. Determination of Thermodynamic Parameters.
For this, the analysis of α vs T was performed for PNIPAm 7k at 15 wt % in H_2O. The variation of the coefficient α with temperature is a signature of the thermal sensitivity of the coil to globule transition. In order to extract the variation of enthalpy involved at the transition, a numerical analysis has been carried out. As this variation of enthalpy can also be reached from the DSC experiments, a comparison between THz spectroscopy and DSC analysis will be performed. As the experiment is reversible, the coil to globule transition has been assumed to obey a simple equilibrium, i.e.,

$$C(H_2O)_n \longleftrightarrow G(H_2O)_{n-q} + qH_2O$$
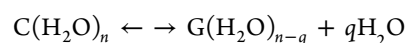
where C is a fully hydrated coil and G a partially hydrated globule, n the number of solvated water molecules per coiled monomer unit, and q the number of water molecules released

into the bulk after the C to G transition. According to the Gibbs free energy law, we have

$$\Delta G^0 = \Delta H^0 - T\Delta S^0 = -RT \ln K \qquad (12)$$

where ΔH^0 is the standard enthalpy of the reaction, S the entropy, R the gas constant, T the temperature, and K the equilibrium constant. The observed variation of α vs T is related to the variation of K as stated by

$$\alpha = \frac{\alpha_1 K + \alpha_2}{1 + K} \qquad (13)$$

where α_1 and α_2 are the values reached by α when K tends to ∞ and K tends to 0, respectively. Due to the presence of these unknown scaling factors, the equilibrium constant K cannot be deduced straightforwardly from the simple observation of the α vs T diagram. A specific numerical technique based on a double derivative must be used (Supporting Information, section 6).[42] This technique allows the determination of the thermodynamic parameters $\Delta H^0/R$ and $\Delta S^0/R$. For PNIPAm 7k at 15 wt % in water: $\Delta H^0/R = (2.3 \pm 0.3) \times 10^4$ K and $\Delta S^0/R = 75 \pm 10$. From these values, the transition temperature can be estimated at 302 ± 2 K. In the same way, the enthalpy of the endothermic C to G transition is 27.3 J·g^{-1} from $(\Delta H^0/R) \times R/M_w$, where R is the gas constant and M_w the molecular weight of the polymer.

The entropy $\Delta S^0/R$ is positive, indicating that the system is less ordered after the transition. However, it is likely that there is compensation between the gain of order of the polymer during the C to G transformation and the gain of disorder when some hydration water molecules are expelled to the bulk. Figure 7 illustrates the validity of the data analysis that has been used
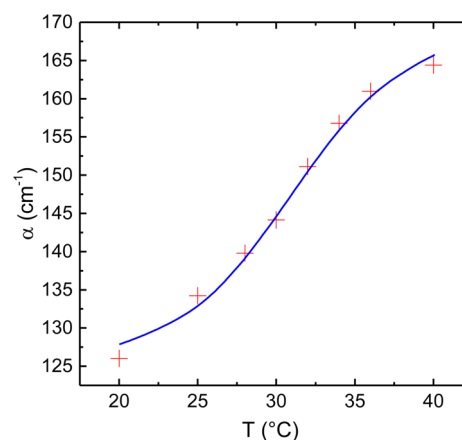

Figure 7. Crosses: experimental of α vs T at 0.8 THz for the P7k15 sample. Solid line: fitting from the model (Supporting Information, section 6.2).

for the determination of the thermodynamic parameters. In order to allow the comparison between THz spectroscopy and DSC, Table 2 gathers the various enthalpies and LCST of the PNIPAm C to G transition as they can be found in the literature or extracted from the provided data. Our results with THz are of the same order of magnitude as the enthalpy found in the literature and confirm the efficiency of this technique to observe thermodynamic behavior during phase transition.

The value of ΔH^0 obtained is in good agreement with the ones observed in the literature issued from DSC measurements. Therefore, despite the limited spectral range of analysis used

Table 2. Comparison of the PNIPAm Coil-to-Globule Enthalpy in Water and LCST Obtained by Various Techniques

PNIPAm coil-to-globule enthalpy in water ΔH (J·g^{-1})	T_c (°C)	M_n (kg mol^{-1})	W (wt %)	solvent	reference
27 ± 3	31.1	7	15	H_2O	this study, THz-TDS[a]
23.3 ± 2.1	32.0	7	15	H_2O	this study, DSC[b]
30.9	29.3	7	20	H_2O	2015, Nguyen[33][c]
18.4 ± 1.2	33.4	7	0.5	H_2O	2015, Nguyen[43][d]
27 ± 3	30.0	12	10	D_2O	2015, Hou[15][e]
47	31.0	44	0.05	H_2O	1990, Otake[44][f]
44	30.8	1600	0.1	H_2O	2005, Ding[45][g]
77	31.8	1600	0.1	H_2O	2005, Ding[45][h]

[a]Data treated with the $r(T)$ method for ΔH (Supporting Information, section S6.2) and with the derivative of the interpolated curve for T_c (Figure S6). [b]ΔH is the average of five values, and T_c is extrapolated at a heating rate of 0 °C·min^{-1} (Supporting Information, section 4.2). [c]DSC measurements during a heating rate of 1 °C·min^{-1}. [d]DSC measurements for ΔH (average of six values) and extrapolated T_c at 0 °C·min^{-1}. [e]From both Van't Hoff plots and our numerical modeling $r(T)$ applied on IR results (Supporting Information, section 6). [f]DSC measurements during a heating rate of +1 °C·min^{-1}. [g]Ultrasensitive DSC (US-DSC) measurements of cooling cycles, then extrapolated values at 0 °C·min^{-1} for ΔH and T_c. [h]US-DSC measurements of heating cycles, then extrapolated values at 0 °C·min^{-1} for ΔH and T_c.

here, reliable ΔH^0 values were inferred from experimental results. Hence, the study of the modifications induced on the hydration shell during the dehydration process is sufficient to have access to information concerning the whole water content. In addition, the consistency of the extracted thermodynamic parameters with the literature data also validates the values of the proposed modification of the hydration number N_h estimated from the curves of Figures 5 and 6, that is ca. 3 water molecules in the case of P7k aqueous solutions with mass fractions W up to 15 wt %.

5. CONCLUSION

We proposed methods to enable the observation of a highly concentrated aqueous solution of PNIPAm and PVCL with THz-TDS transmission measurement before and after the demixing phase transition. In both cases, THz-TDS was able to measure the absorption coefficient of polymer in aqueous solutions and their cloud point temperature. The deviation from ideality, $\Delta\alpha$, revealed to be different depending on the LCST type of the polymer, and gave information on its way to expel water molecules during phase transition. In addition, the comparison between samples showed that concentration had an influence on the $\Delta\alpha$ value, and therefore on the hydration dynamics as well, so it can be predicted and tuned from this knowledge to develop new applications.

Estimated values of the hydration number were given for PNIPAm, based on the assumption that the absorption coefficient of solvation water has a linear evolution with the rise of temperature in the THz range. We observed that our basic estimation predicts for each monomer to lose 3 molecules of water during the phase transition. The rest of the water molecules are either still linked to the polymer at $T > T_c$ or sheltered in the dense network formed by the highly concentrated polymer. Besides, the modification of the absorption coefficient evolution during the phase transition was studied for both PNIPAm and PVCL. We studied the influence of the chain length of the former. In the case of PNIPAm, a methodology to predict the solvation water spectrum was presented and the hydration number evolution was given during the phase transition for temperatures higher than the cloud point, while the polymer is hydrophobic.

A better understanding of the hydration dynamics would require knowing with precision how many water molecules are bound to the polymer molecules. Then, a study of the hydration number evolution after several heating and cooling

processes would be possible in highly concentrated solutions, and would give better insights to understand polymer dynamics in biological environments such as gel-like biological matrixes.[31−35]

Finally, we have shown that THz spectroscopy is an efficient technique to measure the LCST of polymer solutions. Interestingly, it enables an accurate determination of such a temperature from concentrated solution, whereas techniques based on the scattering phenomenon could be hampered by the aggregation−decantation process. With the development of commercially available THz spectrometers, this technique can become another routinely used one for such characterization, bringing a different perspective to the study of the complex processes of LCST.

■ ASSOCIATED CONTENT

ⓢ Supporting Information

The Supporting Information is available free of charge on the ACS Publications website at DOI: 10.1021/acs.jpcb.6b06859.

Polymer characterization (SI1); parameter extraction from THz-TDS, with signal processing of time-domain pulses and frequency domain amplitude and phase to extract the refractive index and absorption coefficient of a sample (SI2); validation of the setup by measurement of the absorption coefficient of pure liquid water in the far-infrared spectra (SI3); cloud point measurement of highly concentrated samples with DSC, THz-TDS, turbidimetry, and DLS (SI4); methodology to calculate the solvation water spectrum and its absorption coefficient α^S (SI5); extraction of the coil-to-globule enthalpy with the numerical method $r(T)$ (SI6); Supporting Information references (SI7) (PDF)

■ AUTHOR INFORMATION

Corresponding Authors
*Phone: (+33) (0)5 61 33 80 77. E-mail: sebastien.massenot@isae-supaero.fr.
*Phone: (+33) (0)5 61 55 62 75. Fax: (+33) (0)5 61 55 62 75. E-mail: coudret@chimie.ups-tlse.fr.

Author Contributions

The manuscript was written through contributions of all authors. All authors have given approval to the final version of manuscript.

■ REFERENCES

(1) Roy, D.; Brooks, W. L. A.; Sumerlin, B. S. New Directions in Thermoresponsive Polymers. *Chem. Soc. Rev.* **2013**, *42*, 7214−7243.

(2) Hoffman, A. S. Stimuli-responsive Polymers: Biomedical Applications and Challenges for Clinical Translation. *Adv. Drug Delivery Rev.* **2013**, *65*, 10−16.

(3) Halperin, A.; Kröger, M.; Winnik, F. M. Poly(N-isopropylacrylamide) Phase Diagrams: Fifty Years of Research. *Angew. Chem., Int. Ed.* **2015**, *54*, 15342−15367.

(4) Meeussen, F.; Nies, E.; Berghmans, H.; Verbrugghe, S.; Goethals, E.; Du Prez, F. Phase Behaviour of Poly(N-vinyl caprolactam) in Water. *Polymer* **2000**, *41*, 8597−8602.

(5) Beija, M.; Marty, J.-D.; Destarac, M. Thermoresponsive Poly(N-vinyl caprolactam)-Coated Gold Nanoparticles: Sharp Reversible Response and Easy Tunability. *Chem. Commun.* **2011**, *47*, 2826−2828.

(6) Zhao, X.; Coutelier, O.; Nguyen, H. H.; Delmas, C.; Destarac, M.; Marty, J.-D. Effect of Copolymer Composition of RAFT/MADIX-derived N-vinylcaprolactam/N-vinylpyrrolidone Statistical Copolymers on Their thermoresponsiveBehavior and Hydrogel Properties. *Polym. Chem.* **2015**, *6*, 5233−5243.

(7) Meeussen, F.; Bauwens, Y.; Moerkerke, R.; Nies, E.; Berghmans, H. Molecular Complex Formation In the System Poly(vinyl methyl ether)/Water. *Polymer* **2000**, *41*, 3737−3743.

(8) Fujishige, S.; Kubota, K.; Ando, I. Phase Transition of Aqueous Solutions of Poly(N-isopropylacrylamide) and Poly(N-isopropylmethacrylamide). *J. Phys. Chem.* **1989**, *93*, 3311−3313.

(9) Chee, C. K.; Rimmer, S.; Soutar, I.; Swanson, L. Fluorescence Investigations of the Thermally Induced Conformational Transition of Poly(N-isopropylacrylamide). *Polymer* **2001**, *42*, 5079−5087.

(10) Balu, C.; Delsanti, M.; Guenoun, P.; Monti, F.; Cloitre, M. Colloidal Phase Separation of Concentrated PNIPAm Solutions. *Langmuir* **2007**, *23*, 2404−2407.

(11) Larsson, A.; Kuckling, D.; Schönhoff, M. 1H NMR of Thermoreversible Polymers in Solution and at Interfaces: the Influence of Charged Groups on the Phase Transition. *Colloids Surf., A* **2001**, *190*, 185−192.

(12) Tauer, K.; Gau, D.; Schulze, S.; Völkel, A.; Dimova, R. Thermal Property Changes of Poly(N-isopropylacrylamide) Microgel Particles and Block Copolymers. *Colloid Polym. Sci.* **2009**, *287*, 299−312.

(13) Shibayama, M.; Mizutani, S.; Nomura, S. Thermal Properties of Copolymer Gels Containing N-Isopropylacrylamide. *Macromolecules* **1996**, *29*, 2019−2024.

(14) Scarpa, J. S.; Mueller, D. D.; Klotz, I. M. Slow Hydrogen-Deuterium Exchange in a non-.alpha.-Helical Polyamide. *J. Am. Chem. Soc.* **1967**, *89*, 6024−6030.

(15) Hou, L.; Wu, P. Comparison of LCST-Transitions of Homopolymer mixture, Diblock and Statistical Copolymers of NIPAM and VCL in Water. *Soft Matter* **2015**, *11*, 2771−2781.

(16) Conti Nibali, V.; Havenith, M. New Insights into the Role of Water in Biological Function: Studying Solvated Biomolecules Using Terahertz Absorption Spectroscopy in Conjunction with Molecular Dynamics Simulations. *J. Am. Chem. Soc.* **2014**, *136*, 12800−12807.

(17) Kongshuang, Z.; Kejuan, H.; Suxiang, W. Progress in the Study of Molecular Organized Assemblies by Dielectric Relaxation Spectroscopy. *Prog. Nat. Sci.* **2006**, *16*, 221−230.

(18) Sun, Y.; Sy, M. Y.; Wang, Y. X.; Ahuja, A. T.; Zhang, Y. T.; Pickwell-Macpherson, E. A Promising Diagnostic Method: Terahertz Pulsed Imaging and Spectroscopy. *World J. Radiol.* **2011**, *3*, 55−65.

(19) McIntosh, A. I.; Yang, B.; Goldup, S. M.; Watkinson, M.; Donnan, R. S. Terahertz Spectroscopy: a Powerful new Tool for the Chemical Sciences? *Chem. Soc. Rev.* **2012**, *41*, 2072−2082.

(20) Rønne, C.; Thrane, L.; Åstrand, P.-O; Wallqvist, A.; Mikkelsen, K. V.; Keiding, S. R. Investigation of the Temperature Dependence of Dielectric Relaxation in Liquid Water by THz Reflection Spectroscopy and Molecular Dynamics Simulation. *J. Chem. Phys.* **1997**, *107*, 5319−5331.

(21) Matvejev, V.; Zizi, M.; Stiens, J. Hydration Shell Parameters of Aqueous Alcohols: THz Excess Absorption and Packing Density. *J. Phys. Chem. B* **2012**, *116*, 14071−14077.

(22) Leitner, D. M.; Gruebele, M.; Havenith, M. Solvation Dynamics of Biomolecules: Modeling and Terahertz Experiments. *HFSP J.* **2008**, *2*, 314−323.

(23) Born, B.; Havenith, M. Terahertz Dance of Proteins and Sugars with Water. *J. Infrared, Millimeter, Terahertz Waves* **2009**, *30*, 1245−1254.

(24) Born, B.; Weingärtner, H.; Bründermann, E.; Havenith, M. Solvation Dynamics of Model Peptides Probed by Terahertz Spectroscopy. Observation of the Onset of Collective Network Motions. *J. Am. Chem. Soc.* **2009**, *131*, 3752−3755.

(25) Wallace, V. P.; Ferachou, D.; Ke, P.; Day, K.; Uddin, S.; Casas-Finet, J.; Van Der Walle, C. F.; Falconer, R. J.; Zeitler, J. A. Modulation of the Hydration Water Around Monoclonal Antibodies on Addition of Excipients Detected by Terahertz Time-Domain Spectroscopy. *J. Pharm. Sci.* **2015**, *104*, 4025−4033.

(26) Naito, H.; Ogawa, Y.; Hoshina, H.; Sultana, S.; Kondo, N. Analysis of Intermolecular Interaction of Poly(N-isopropylacrylamide) Solution with Attenuated Total Reflection Terahertz Spectroscopy. *Appl. Phys. Lett.* **2012**, *100*, 191102.

(27) Shiraga, K.; Naito, H.; Suzuki, T.; Kondo, N.; Ogawa, Y. Hydration and Hydrogen Bond Network of Water during the Coil-to-Globule Transition in Poly(N-isopropylacrylamide) Aqueous Solution at Cloud Point Temperature. *J. Phys. Chem. B* **2015**, *119*, 5576−5587.

(28) Ono, Y.; Shikata, T. Hydration and Dynamic Behavior of Poly(N-isopropylacrylamide)s in Aqueous Solution: A Sharp Phase Transition at the Lower Critical Solution Temperature. *J. Am. Chem. Soc.* **2006**, *128*, 10030−10031.

(29) Füllbrandt, M.; Ermilova, E.; Asadujjaman, A.; Hölzel, R.; Bier, F. F.; von Klitzing, R.; Schönhals, A. Dynamics of Linear Poly(N-isopropylacrylamide) in Water around the Phase Transition Investigated by Dielectric Relaxation Spectroscopy. *J. Phys. Chem. B* **2014**, *118*, 3750−3759.

(30) Vorob'ev, M. M.; Burova, T. V.; Grinberg, N. V.; Dubovik, A. S.; Faleev, N. G.; Lozinsky, V. I Hydration Characterization of N-vinylcaprolactam Polymers by Absorption Millimeter-wave Measurements. *Colloid Polym. Sci.* **2010**, *288*, 1457−1463.

(31) Bagchi, B. Water Dynamics in the Hydration Layer around Proteins and Micelles. *Chem. Rev.* **2005**, *105*, 3197−3219.

(32) Ball, P. Water as an Active Constituent in Cell Biology. *Chem. Rev.* **2008**, *108*, 74−108.

(33) Nguyen, H. H.; Payré, B.; Fitremann, J.; Lauth-de Viguerie, N.; Marty, J.-D. Thermoresponsive Properties of PNIPAM-Based Hydrogels: Effect of Molecular Architecture and Embedded Gold Nanoparticles. *Langmuir* **2015**, *31*, 4761−4768.

(34) Heugen, U.; Schwaab, G.; Bründermann, E.; Heyden, M.; Yu, X.; Leitner, D. M.; Havenith, M. Solute-Induced Retardation of Water Dynamics Probed Directly by Terahertz Spectroscopy. *Proc. Natl. Acad. Sci. U. S. A.* **2006**, *103*, 12301−12306.

(35) Shibayama, M.; Morimoto, M.; Nomura, S. Phase Separation Induced Mechanical Transition of Poly(N-isopropylacrylamide)/Water Isochore Gels. *Macromolecules* **1994**, *27*, 5060−5066.

(36) Kogure, H.; Nanami, S.; Masuda, Y.; Toyama, Y.; Kubota, K. Hydration and Dehydration Behavior of N-isopropylacrylamide Gel Particles. *Colloid Polym. Sci.* **2005**, *283*, 1163−1171.

(37) Ono, Y.; Shikata, T. Contrary Hydration Behavior of N-Isopropylacrylamide to its Polymer, P(NIPAm), with a Lower Critical Solution Temperature. *J. Phys. Chem. B* **2007**, *111*, 1511−1513.

(38) Heyden, M.; Sun, J.; Funkner, S.; Mathias, G.; Forbert, H.; Havenith, M.; Marx, D. Dissecting the THz Spectrum of Liquid Water from First Principles via Correlations in Time and Space. *Proc. Natl. Acad. Sci. U. S. A.* **2010**, *107*, 12068−12073.

(39) Chassenieux, C.; Nicolai, T.; Durand, D. Association of Hydrophobically End-Capped Poly(ethylene oxide). *Macromolecules* **1997**, *30*, 4952−4958.

(40) Kubota, K.; Hamano, K.; Kuwahara, N.; Fujishige, S.; Ando, I. Characterization of Poly(N-isopropylmethacrylamide) in Water. *Polym. J.* **1990**, *22*, 1051−1057.

(41) Lele, A. K.; Hirve, M. M.; Badiger, M. V.; Mashelkar, R. A. Predictions of Bound Water Content in Poly(N-isopropylacrylamide) Gel. *Macromolecules* **1997**, *30*, 157−159.

(42) Tan-Sien-Hee, L.; Lavabre, D.; Levy, G.; Micheau, J. C. Multiwavelength Analysis of Thermochromic Equilibria Application to the [Ni(tmen) (acac)]+ Ion in Different Solvents. *New J. Chem.* **1989**, *13*, 227−233.

(43) Nguyen, H. H.; Brûlet, A.; Goudounèche, D.; Saint-Aguet, P.; Lauth-de Viguerie, N.; Marty, J.-D. The Effect of Polymer Branching and Average Molar Mass on the Formation, Stabilization and Thermoresponsive properties of Gold Nanohybrids Stabilized by Poly(N-isopropylacrylamide). *Polym. Chem.* **2015**, *6*, 5838−5850.

(44) Otake, K.; Inomata, H.; Konno, M.; Saito, S. Thermal Analysis of the Volume Phase Transition with N-isopropylacrylamide Gels. *Macromolecules* **1990**, *23*, 283−289.

(45) Ding, Y.; Ye, X.; Zhang, G. Microcalorimetric Investigation on Aggregation and Dissolution of Poly(N-isopropylacrylamide) Chains in Water. *Macromolecules* **2005**, *38*, 904−908.